CHIN. PHYS. LETT. Vol. 37, No. 9 (2020) 097802 **Express Letter**

Ultrafast Quasiparticle Dynamics and Electron-Phonon Coupling in $(Li_{0.84}Fe_{0.16})OHFe_{0.98}Se$

Qiong Wu(吴穹)[1,2], Huaxue Zhou(周花雪)[1], Yanling Wu(吴艳玲)[1], Lili Hu(胡立立)[1], Shunli Ni(倪顺利)[1,2], Yichao Tian(田义超)[1], Fei Sun(孙飞)[1,2], Fang Zhou(周放)[1,2,3], Xiaoli Dong(董晓莉)[1,2,3], Zhongxian Zhao(赵忠贤)[1,2,3], and Jimin Zhao(赵继民)[1,2,3*]

[1]*Beijing National Laboratory for Condensed Matter Physics, Institute of Physics, Chinese Academy of Sciences, Beijing 100190, China*

[2]*School of Physical Sciences, University of Chinese Academy of Sciences, Beijing 100049, China*

[3]*Songshan Lake Materials Laboratory, Dongguan 523808, China*

(Received 18 July 2020; accepted 9 August 2020; published online)

Distinctive superconducting behaviors between bulk and monolayer FeSe make it challenging to obtain a unified picture of all FeSe-based superconductors. We investigate the ultrafast quasiparticle (QP) dynamics of an intercalated superconductor $(Li_{1-x}Fe_x)OHFe_{1-y}Se$, which is a bulk crystal but shares a similar electronic structure with single-layer FeSe on $SrTiO_3$. We obtain the electron-phonon coupling (EPC) constant $\lambda_{A_{1g}}$ (0.22 ± 0.04), which well bridges that of bulk FeSe crystal and single-layer FeSe on $SrTiO_3$. Significantly, we find that such a positive correlation between $\lambda_{A_{1g}}$ and superconducting T_c holds among all known FeSe-based superconductors, even in line with reported FeAs-based superconductors. Our observation indicates possible universal role of EPC in the superconductivity of all known categories of iron-based superconductors, which is a critical step towards achieving a unified superconducting mechanism for all iron-based superconductors.

PACS: 78.47.J−, 78.47.jg, 71.38.−k, 74.70.−b DOI: 10.1088/0256-307X/37/9/097802

Most high-temperature superconductors exhibit quasi-two-dimensional superconducting (SC) layers. However, a unified physical picture of the FeSe-based[1] and FeAs-based superconductors[2] remains elusive thus far, regardless of the common layered feature they share. The recent discoveries of single-layer FeSe (on $SrTiO_3$ or similar substrates) interface superconductors[3] and $(Li_{1-x}Fe_x)OHFe_{1-y}Se$ intercalated superconductors[4] seemingly reinforced this uncertainty. However, by examining these newly discovered crucial types of superconductors, possible connections among all categories of iron-based superconductors can be uncovered, leading towards a universal picture of them all.

In this Letter, we investigate the electron-phonon coupling (EPC) strength in these superconductors by using ultrafast spectroscopy[5−12] to gain insights into a unified understanding of iron-based superconductors. We probe the excited state QP dynamics of a bulk crystal $(Li_{0.84}Fe_{0.16})OHFe_{0.98}Se$,[13] which allows direct observation of the QP lifetimes, uncovering the phenomena above the SC gap and across the SC transition. Light pulses break the Cooper pairs and generate excited-state nonequilibrium QPs, which recombine with a lifetime determined mainly by the EPC.[5,6] The stronger the EPC, the faster the energy transfer through EPC, and hence the shorter lifetime. We determine the EPC strength to be $\lambda_{A_{1g}} = 0.22 \pm 0.04$, which is larger than that of bulk FeSe $(\lambda_{A_{1g}} = 0.16)$[5] and smaller than that of single-layer $FeSe/SrTiO_3$ $(\lambda_{A_{1g}} = 0.48)$.[6]

$(Li_{1-x}Fe_x)OHFe_{1-y}Se$ crystals[4,13,14] consist of staggered stack of $Fe_{1-y}Se$ and $(Li_{1-x}Fe_x)OH$ layers, whose structure is analogous to that of $K_xFe_2Se_2$,[15] but with the $P4/nmm$ space group instead of the $I4/mmm$ space group. The electronic band structure of $(Li_{1-x}Fe_x)OHFe_{1-y}Se$ is similar to that of single-layer $FeSe/SrTiO_3$[16] and bulk $Rb_xFe_{2-y}Se_2$.[17] As a result, $(Li_{1-x}Fe_x)OHFe_{1-y}Se$ forms a key bridge between bulk FeSe, $A_xFe_{2-y}Se_2$ (A = K, Rb, Cs, Tl/K), and single-layer $FeSe/SrTiO_3$ superconductors. To some extent, $(Li_{1-x}Fe_x)OHFe_{1-y}Se$ provides an excellent platform for gaining insights into the shared SC origin of these materials.[13,16−18]

In this work, we demonstrate that the $\lambda_{A_{1g}}$ value of $(Li_{1-x}Fe_x)OHFe_{1-y}Se$ bridges those of bulk FeSe, $Fe_{1.01}Se_{0.2}Te_{0.8}$, $Fe_{1.05}Se_{0.2}Te_{0.8}$, $K_xFe_2Se_2$ and single-layer $FeSe/SrTiO_3$. Significantly, by examin-

Supported by the National Key Research and Development Program of China (Grant Nos. 2017YFA0303603 and 2016YFA0300300), the National Natural Science Foundation of China (Grant Nos. 11574383, 11774408, and 11574370), the Frontier Program of the Chinese Academy of Sciences (Grant No. QYZDY-SSW-SLH001), the Strategic Priority Research Program of CAS (Grant No. XDB30000000), the Beijing Natural Science Foundation (Grant No. 4191003), the International Partnership Program of Chinese Academy of Sciences (Grant No. GJHZ1826), and CAS Interdisciplinary Innovation Team.

*Corresponding author. Email: jmzhao@iphy.ac.cn

ing this and the reported $\lambda_{A_{1g}}$ values measured using ultrafast spectroscopy for many FeSe-based and FeAs-based superconductors, as well as those calculated in theory, we find a positive correlation between the EPC strength $\lambda_{A_{1g}}$ and the SC transition temperature T_c. Our results indicate the possible important role of EPC in the superconductivity for all categories of iron-based superconductors, thus contributing to a unified understanding of the SC mechanism.

Experiments. Ultrafast laser pulses with a central wavelength of 800 nm, 70 fs pulse width and 250 kHz repetition rate are used to excite and probe the dynamics of QPs, as well as to generate and detect coherent phonons, in a $(Li_{0.84}Fe_{0.16})OHFe_{0.98}Se$ single crystal, along with two other samples of $Fe_{1.05}Se_{0.2}Te_{0.8}$ and $Fe_{1.01}Se_{0.2}Te_{0.8}$. The time-resolved pump-probe weak detection experimental setup is similar to that of Ref. [6]. Moreover, a balanced detector is used to further improve the signal-to-noise ratio. Our sample is synthesized via a hydrothermal ion-exchange technique (with SC $T_c = 40$ K), the details of which have been described in Ref. [13]. The measured sample is $1.2 \times 2\,mm^2$-sized, composing of micron-sized single-crystal flakes, and is kept in a refrigerator to prevent degradation before and after the experiments. Its surface is not entirely optical flat, resulting in diffusive reflections, which makes it challenging to collect the reflected beam and further to obtain useful signals.

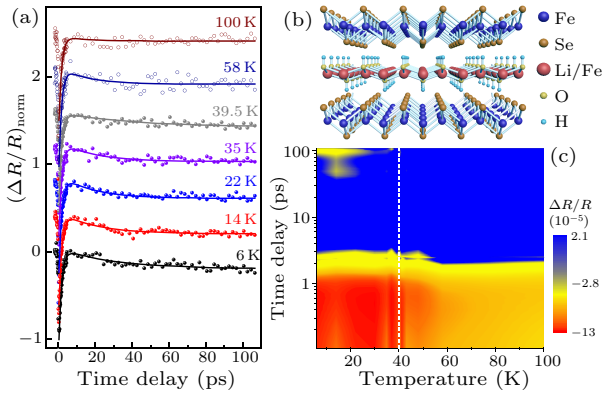

Fig. 1. Ultrafast QP dynamics in $(Li_{0.84}Fe_{0.16})OHFe_{0.98}Se$. (a) Normalized time-resolved differential reflectivity $\Delta R/R$ at different temperatures (offset for clarity). Spheres: scanning data below SC T_c; open circles: scanning data above SC T_c; solid curves: 2-exponential fittings. (b) Schematic lattice structure with $P4/nmm$ symmetry. (c) Color map of $\Delta R/R$ as a function of both the delay time and temperature. The color change at 40 K reveals a likely SC phase transition (indicated by a white dashed line).

Ultrafast QP Dynamics Revealing the SC Properties. Figure 1(a) shows the differential reflectivity $\Delta R/R$ of our $(Li_{0.84}Fe_{0.16})OHFe_{0.98}Se$ sample (data are offset for clarity), with the schematic crystal structure illustrated in Fig. 1(b), where the pump fluence is 21 μJ/cm^2 and probe fluence is 8.2 μJ/cm^2. The $\Delta R/R$ is proportional to the density of the excited state QPs. We color-map the complete set of data as a function of both temperature and time delay in Fig. 1(c) (on the logarithmic scale for clarity). The color change exhibits a phase transition at 40 K, which is similar to those SC transitions in monolayer FeSe superconductor[6] and many others.[10] The phase transition temperature 40 K is also consistent with the reported SC T_c for $(Li_{1-x}Fe_x)OHFe_{1-y}Se$ by other experimental methods.[4,13,14,18]

To further verify the SC transition, we quantitatively analyze the data in Fig. 1(c) using $\Delta R/R = A_{fast}\exp(-t/\tau_{fast}) + A_{slow}\exp(-t/\tau_{slow}) + y_0$, where A_{fast} (A_{slow}) and τ_{fast} (τ_{slow}) are the amplitude and lifetime of the fast (slow) component, respectively. The fast relaxation component mainly reflects the EPC, and the slow component mainly reflects the phonon-phonon scattering. The third term y_0 is a constant within the scanning range and slightly varies with temperature. Indeed, it may be a component with a lifetime much longer than the scanning range,[5,19] which could be due to scatterings among acoustic phonons. We mainly focus on the fast and slow components.

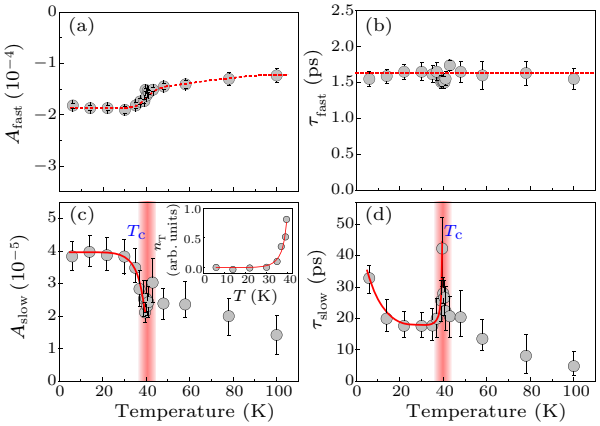

Fig. 2. Quantitative QP dynamic evidence of the SC phase transition. [(a), (b)] Amplitude A_{fast} and lifetime τ_{fast} of the fast relaxation component and their temperature dependence. [(c), (d)] Amplitude A_{slow} and lifetime τ_{slow} of the slow relaxation component and their temperature dependence. Inset: thermal carrier density. Red solid curves in (c) and (d) show the theoretical data fitting based on the phenomenological Rothwarf–Taylor model. Dashed curves in (a) and (b) are the visual guides. Red vertical bars in (c) and (d) show the temperature region where SC phase transition occurs.

We then investigate the temperature dependence of the QP dynamics. Figure 2(a) shows that A_{fast} behaves similarly to that of single-layer FeSe/$SrTiO_3$.[6] Figure 2(b) demonstrates that τ_{fast} is nearly a constant for the whole temperature range. Figure 2(c) exhibits that A_{slow} experiences a dramatic decrease near 39.5 K, similar to those in monolayer FeSe/$SrTiO_3$[6]

and other superconductors.[20] Figure 2(d) illustrates that $\tau_{\rm slow}$ forms a peak (i.e., enhanced QP lifetime) at 39.5 K, directly manifesting the well-known phonon bottleneck effect.[6,21] The simultaneous observation of the abrupt decrease in the amplitude [Fig. 2(c)] and the lifetime maximum [Fig. 2(d)] at the same temperature indicates an SC phase transition.[6,20] To further verify this, we quantitatively analyze the temperature dependence of $A_{\rm slow}$ and $\tau_{\rm slow}$ (see the Supplementary Material) by using the Rothwarf–Taylor (RT) model[22] and its extended derivation.[23] The curves based on this model for a superconductor are plotted in Figs. 2(c) and 2(d) (red solid curves), respectively, both revealing $T_{\rm c} = 39.7 \pm 0.5$ K and the SC gap $\Delta(0) = 14.3 \pm 1.2$ meV. The density of thermally excited QPs, $n_{\rm T}$, is also illustrated in the inset of Fig. 2(c). We thus identify $\Delta(0)/k_{\rm B}T_{\rm c}$ to have a value of 4.1, which is much larger than the BCS prediction $\Delta(0)/k_{\rm B}T_{\rm c} = 1.76$. Here the evidence and parameters of the SC transition are obtained by probing the excited-state ultrafast dynamics, rather than by measuring the equilibrium near-Fermi-surface properties. The results in Figs. 1 and 2 are obtained within the weak detection regime. By weak detection, we propose two different levels of criteria: (A) no thermal effect and (B) no prominent destruction of the SC component (see the Supplementary Material), which are both fulfilled in obtaining Figs. 1 and 2.

Obtaining the EPC Strength λ or $\lambda_{A_{1g}}$. By measuring the QP ultrafast dynamics under relatively high excitation laser fluence, the EPC constant λ can be directly obtained.[24] In the Allen model, which can be applied to both superconductors and most other solids, the relaxation rate $\gamma_{\rm T}$ of the QPs is determined jointly by the EPC constant λ and the electron temperature $T_{\rm e}$ in a relation

$$\gamma_{\rm T} = \frac{3\hbar\lambda\langle\Omega^2\rangle}{\pi k_{\rm B}T_{\rm e}}\left[1 - \frac{\hbar^2\langle\Omega^4\rangle}{12\langle\Omega^2\rangle k_{\rm B}^2 T_{\rm e}T_{\rm L}} + \cdots\right],$$

where $\lambda\langle\Omega^2\rangle$ is the second moment of the Eliashberg function, $T_{\rm L}$ is the lattice temperature, and Ω is the phonon frequency. We measure the electron temperature $T_{\rm e}$ and the QP relaxation rate $\gamma_{\rm T}$ in our ultrafast dynamics experiment.

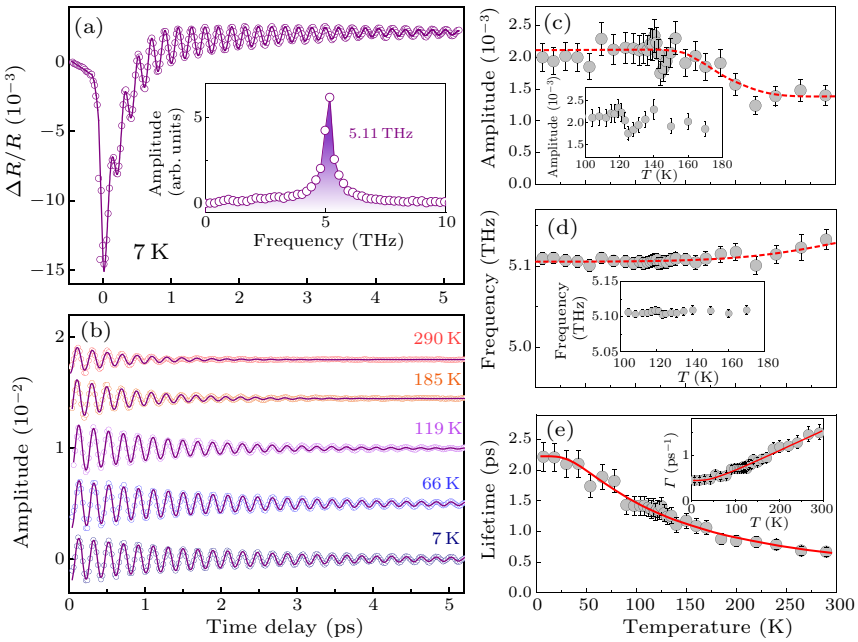

Fig. 3. High fluence ultrafast dynamics (based on which we obtain the value of λ) and coherent optical phonon. (a) Time-resolved coherent optical phonon vibration at 7 K, which is superimposed on the electronic relaxation. Inset: the fast Fourier transform result showing a clear peak at 5.11 THz. The pump fluence is 2.2 mJ/cm^2. (b) Extracted phonon oscillations at several temperatures. (c)–(e) Temperature dependence of the phonon amplitude, frequency, and lifetime. Dashed curves: visual guides. Solid curves: anharmonic decay fitting results. Insets in (c)–(e): magnified views and the corresponding phonon decay rate Γ (i.e., 1/lifetime).

We employ the data shown in Fig. 3(a) to obtain λ (or $\lambda_{A_{1g}}$, see following paragraphs). Note that obtaining λ does not need weak detection condition or low temperature environment, because EPC is a fundamental property of solids and does not rely on superconductivity. In the Supplementary Material, we demonstrate that λ is nearly a constant of both fluence and temperature in high fluence regime.

To obtain $T_{\rm e}$, note that the high order terms in the equation of $\gamma_{\rm T}$ are negligible only when $T_{\rm e}T_{\rm L}$ is relatively large. This condition is fulfilled in our high-fluence excitation experiments, with the pump fluence $F = 2.2$ mJ/cm^2 (and probe fluence 0.28 mJ/cm^2) [Fig. 3(a)]. We calculate $T_{\rm e}$ using the relation[5,25]

$$T_{\rm e} = \left\langle \sqrt{T_{\rm L}^2 + \frac{2(1-R)F}{\kappa_{\rm v} l_{\rm s}} e^{-z/l_{\rm s}}} \right\rangle,$$

where $l_{\rm s}$ is the optical penetration depth, z is the distance from the sample surface, and $\kappa_{\rm v} = \kappa\rho_{\rm n}$ is the electronic heat capacity coefficient for unit volume, with κ being the electronic heat capacity coefficient (Sommerfeld parameter) and $\rho_{\rm n}$ being the mole density (see the Supplementary Material). By interpreting $\kappa = 100\,{\rm mJ/(mol\cdot K^2)}$ from Ref. [4] and taking $T_{\rm L} = 7\,{\rm K}$, we obtain $T_{\rm e} = 548\,{\rm K}$. Because $T_{\rm L}$ only affects $T_{\rm e}$ less than a few Kelvin (when $T_{\rm L}$ is relatively low), $T_{\rm e}$ is close to a constant (see the Supplementary Material).

The relaxation rate is defined as[24]

$$\gamma_{\rm T} = \left| \frac{1}{T_{\rm e} - T_{\rm L}} \frac{d(T_{\rm e} - T_{\rm L})}{dt} \right|_{t\to 0}.$$

It is known that $(T_{\rm e} - T_{\rm L}) \propto \Delta R/R$.[26] Furthermore, at $t \to 0$, the fast component dominates. Thus we have

$$\gamma_{\rm T} = \left| \frac{1}{\Delta R} \frac{d(\Delta R)}{dt} \right|_{t\to 0} \approx \frac{1}{\tau_{\rm fast}}.$$

Fitting the electronic dynamics (after subtracting the overall dynamics of phonon oscillations) at $T_{\rm L} = 7\,{\rm K}$ [Fig. 3(a)], after performing deconvolution, we obtain $\tau_{\rm fast} = 0.34 \pm 0.05\,{\rm ps}$ (see the Supplementary Material). Thus, $\gamma_{\rm T} = 1/\tau_{\rm fast} = 2.9 \pm 0.5\,{\rm ps}^{-1}$. The $\tau_{\rm fast}$ is longer than the 0.23 ps lifetime of single-layer FeSe/$SrTiO_3$ system[6] and shorter than the 1.75 ps lifetime of bulk FeSe.[5] Note that in the medium[27] and high fluence[9] regime, $\tau_{\rm fast}$ increases with fluence, whereas the value of λ remains constant (see the Supplementary Material). With the above observed values of $T_{\rm e}$ and $\gamma_{\rm T}$ we derive $\lambda\langle\Omega^2\rangle = 2.34 \times 10^{26}\,{\rm Hz}^2$ (i.e., $101\,{\rm meV}^2$).

The phonon information is needed for obtaining λ. We generate and detect coherent phonons[28–32] in $(Li_{0.84}Fe_{0.16})OHFe_{0.98}Se$ with identical high fluence as shown by the data in Fig. 3(a). We extract the coherent oscillation and perform Fourier transformation to obtain its frequency [Fig. 3(a) inset], which is 5.11 THz (i.e., 21.2 meV or $171\,{\rm cm}^{-1}$). We assign it to be the A_{1g} mode of the Se atoms, which corresponds to layer breathing along the c-axis. The temperature dependence of the coherent phonon is investigated [Figs. 3(b)–3(e)], which exhibits a regular anharmonic phonon decay[28] [Fig. 3(e)]. Figures 3(c)–3(e) show that there is no structural phase transition in the temperature range of 100–180 K. If we use the above measured A_{1g} phonon frequency, 21.2 meV, we can obtain a *nominal* EPC constant $\lambda_{A_{1g}} = 0.22 \pm 0.04$.

Distinguishing EPC Strength λ with $\lambda_{A_{1g}}$. Note that demonstrating the A_{1g} phonon does not indicate that the A_{1g} mode phonon is exactly the pairing glue. So far, there is no consensus on which phonon mode contributes most to the EPC strength λ. In fact, nominal values of $\lambda_{A_{1g}}$ in superconductors are frequently reported, however, in the name of λ.[5,6,9,33,34] Here, we clearly distinguish $\lambda_{A_{1g}}$ and λ, which clearly illustrates important basic facts that are otherwise mixed, concealing important conclusions. We find that (A) by distinguishing $\lambda_{A_{1g}}$ and λ, we are now able to compare better the (many reported) experimental results with theoretical calculations; (B) the values of $\lambda_{A_{1g}}$ are all based on experimental facts, thus deserve consideration and comparison; and (C) significantly, both $\lambda_{A_{1g}}$ and λ exhibit positive correlations with $T_{\rm c}$, but not when $\lambda_{A_{1g}}$ and λ are mixed.

Table 1. Retrieval of $\lambda_{A_{1g}}$ from the theoretical values of λ.

Material	$\Omega_{\log}$ ($\rm cm^{-1}$)	λ	$\Omega_{A_{1g}}$ ($\rm cm^{-1}$)	$(\Omega_{\log}/\Omega_{A_{1g}})^2$	$\lambda_{A_{1g}}$	$T_{\rm c}$(K)
FeSe	113[35]	0.17[35]	180[36]	0.394	0.067	8
NaFeAs	100[37]	0.27[37]	163[38]	0.376	0.1	9
$FeSe_{0.5}Te_{0.5}$	110[39]	0.3[39]	170	0.419	0.13	14.5
$LaFe_{1.85}AsO_{0.875}F_{0.125}$	141[40]	0.35	201[41]	0.46	0.16[42]	26
$CaFe_{1.85}Co_{0.15}As_2$	107[43]	0.36[43]	189[44]	0.321	0.115	16
LiFeAs	120[37]	0.29[37]	185[45]	0.42	0.12	18
$K_xFe_2Se_2$	125[46]	0.34[46]	174[47]	0.516	0.175	30
$Ba_{0.6}K_{0.4}Fe_2As_2$	124[48]	0.47[48]	187[49]	0.44	0.207	38

The values of $\lambda_{A_{1g}}$ and λ can be related (converted into each other) by the relation $\lambda_{A_{1g}} = \lambda(\Omega_{\log}^2/\Omega_{A_{1g}}^2)$, which we derive based on Refs. [24,50,51]. Here we define $\lambda\langle\Omega^2\rangle \equiv \lambda_{A_{1g}}\langle\Omega_{A_{1g}}^2\rangle = \lambda_{A_{1g}}\Omega_{A_{1g}}^2$, where $\lambda_{A_{1g}}$ is the nominal EPC strength corresponding to the A_{1g} mode phonon. Based on the Allen–Dynes treatment, logarithmic phonon frequency $\Omega_{\log}$ is taken to be the overall average,[50] thus we write $\lambda\langle\Omega^2\rangle = \lambda\langle\Omega_{\log}^2\rangle = \lambda\Omega_{\log}^2$. Combining both of them, we retrieve the values of $\lambda_{A_{1g}}$ by using $\lambda_{A_{1g}} = \lambda(\Omega_{\log}^2/\Omega_{A_{1g}}^2)$. The detailed values are summarized in Table 1.

Universal Role of EPC in Iron-Based Superconductors. The EPC has been speculated to play an active role in certain individual types of iron-based high-$T_{\rm c}$ superconductors, particularly such as the single-layer system.[3,6,52] Here we contemplate on *all* categories of iron-based superconductors. We plot the available $T_{\rm c}$ versus $\lambda_{A_{1g}}$ for different optimally doped iron-based

superconductors in Fig. 4 (for detailed values, see Table 2).

To avoid systematic discrepancies due to different experimental methods, we mainly summarize experimental $\lambda_{A_{1g}}$ values obtained by using time-resolved ultrafast optical spectroscopy (including time-resolved angle-resolved photoemission spectroscopy, red spheres and squares),[5,6,8,9,53] as well as theoretical results (blue spheres and squares).[35,37,39,42,43,46,48] Note that some of the data are retrieved by the authors (see the Supplementary Material). Furthermore, we perform ultrafast optical spectroscopy experiments on $Fe_{1.05}Se_{0.2}Te_{0.8}$ ($T_c = 10$ K) and $Fe_{1.01}Se_{0.2}Te_{0.8}$ ($T_c = 13.5$ K) single crystals, and obtain the $\lambda_{A_{1g}}$ values to be 0.11 and 0.13, respectively (see the Supplementary Material).

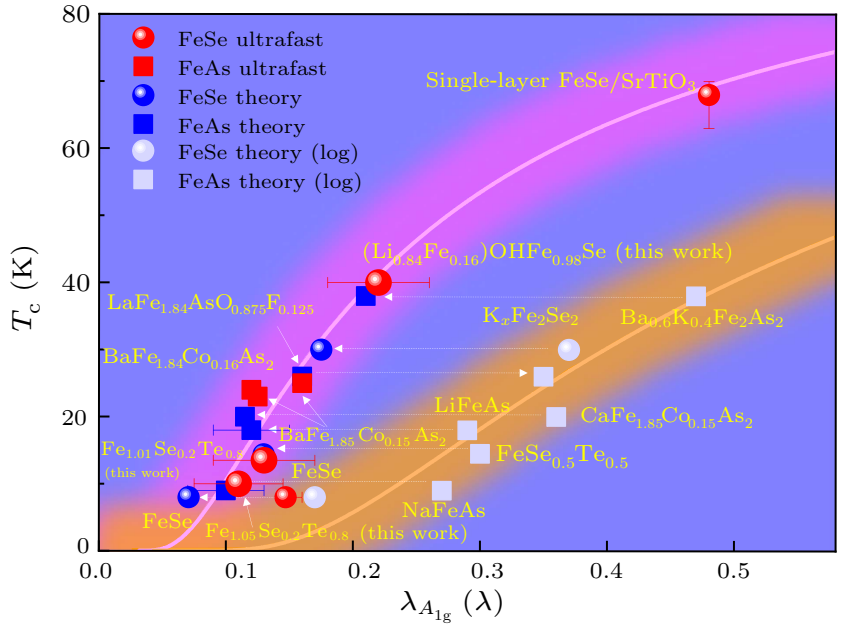

Fig. 4. Positive correlation between the EPC strength $\lambda_{A_{1g}}$ (λ) and SC T_c in iron-based superconductors. The SC T_c positively correlates to the EPC strength $\lambda_{A_{1g}}$ (λ). Red spheres (squares): ultrafast spectroscopy results of FeSe (FeAs)-based superconductors (three data from this work and Refs. [5,6,8,9,53]). Blue sphere (squares): retrieved theoretical calculation results of FeSe (FeAs)-based superconductors.[35,37,39,42,43,46,48] Light gray spheres (squares): theoretical results of λ for FeSe (FeAs)-based superconductors. Pink (orange) curve: ansatz modified version of Allen–Dynes formula using $\lambda_{A_{1g}}$ (λ) and $\Omega_{A_{1g}}$ ($\Omega_{\log}$). White dashed arrows: indications of retrieving $\lambda_{A_{1g}}$ from λ, or vise versa.

Table 2. The T_c and $\lambda_{A_{1g}}$ values of iron-based superconductors shown in Fig. 4.

Superconductors	T_c (K)	$\lambda_{A_{1g}}$
Bulk FeSe	8[1]	0.07 (retrieved from Ref. [35])
Bulk FeSe	8[1]	0.14 (retrieved from Ref. [5])
NaFeAs	9[54]	0.1 (retrieved from Ref. [37])
$Fe_{1.05}Se_{0.2}Te_{0.8}$	10 (this work)	0.11 ± 0.03 (this work)
$Fe_{1.01}Se_{0.2}Te_{0.8}$	13.5 (this work)	0.13 ± 0.03 (this work)
$FeSe_{0.5}Te_{0.5}$	14.5[55]	0.13 (retrieved from Ref. [39])
LiFeAs	18[56]	0.12 (retrieved from Ref. [37])
$CaFe_{1.85}Co_{0.15}As_2$	20[43]	0.115 (retrieved from Ref. [43])
$BaFe_{1.85}Co_{0.15}As_2$	23[53]	0.125[53]
$BaFe_{1.84}Co_{0.16}As_2$	24[9]	0.12[9]
$BaFe_{1.85}Co_{0.15}As_2$	25[8]	0.16[8]
$LaFe_{1.85}AsO_{0.875}F_{0.125}$	26[2]	0.16[42]
$K_xFe_2Se_2$	30[15]	0.175 (retrieved from Ref. [46])
$Ba_{0.6}K_{0.4}Fe_2As_2$	38[48]	0.21 (retrieved from Ref. [48])
$(Li_{0.84}Fe_{0.16})OHFe_{0.98}Se$	39.7 ± 0.5 (this work)	0.22 ± 0.04 (this work)
1UC FeSe/$SrTiO_3$	68(−5/+2)[6]	0.48[6]

Significantly, all the $\lambda_{A_{1g}}$ data points are located within a purple stripe region centered on a pink curve in Fig. 4, indicating a positive correlation between T_c and $\lambda_{A_{1g}}$. The pink curve is a revised version of the Allen–Dynes formula,[50] based on $\lambda_{A_{1g}}$ and $\Omega_{A_{1g}}$ (see the Supplementary Material). Similarly, we also plot available reported theoretical results of λ in Fig. 4 (marked by light gray squares or spheres), which are located within a brown stripe region centered on an orange curve (another revised version of the Allen–Dynes formula, based on λ and $\Omega_{\log}$) (see the Supplementary Material). Because $\lambda_{A_{1g}}$ and λ are explicitly distinguished here, and EPC is considered systematically for the whole family of iron-based superconductors, we are able to establish a hitherto unrecognized correlation between T_c and $\lambda_{A_{1g}}$ (λ) for iron-based superconductors, using all the theoretical and experimental results available. We emphasize that the positive correlation itself, rather than the details of the fitting equations, is the most significant finding. The modification of the Allen–Dynes formula can be attributed to complex systematic discrepancies among different experimental methods. For instance, there may be a systematic discrepancy between experimental results based on nonequilibrium excited-state photo-carrier relaxation and those based on equilibrium ground-state electron tunneling.

Discussion. Remarkably, bulk, single-layer, and intercalated iron-based superconductors all obey these two correlations, and both FeSe- and FeAs-based superconductors obey the same correlations as well (Fig. 4). This observation strongly suggests that a shared SC origin is ubiquitous in all categories of iron-based superconductors, whereby the EPC plays a universal role. We speculate that such EPC may not be a conventional type of EPC. Moreover, we do not rule out other origins in making important contributions to the SC mechanism (for instance, spin interactions or charge modulations may affect the EPC through modifying the electronic states or the phonons). Various types of excitations, interactions, modifications, or perturbations may affect either the electron states, or the phonons, or both of them. As a result, each of them will lead to the modification of the EPC strength. Therefore, they will also possibly modify the SC properties, in an indirect way through the EPC (for example, see the illustration in the Supplementary Material). Hence, it is better to measure the EPC (preferably also phonon properties) before excluding phonons as the pairing glue.

We note that it is very unlikely what we measure is not EPC but other e-boson coupling (or a sum of them). (1) We did not use circular polarization pump and probe geometries in our experiment, which are often needed for detecting fast magnetic or spin-related dynamics. (2) The QP lifetimes due to phonons and other glues must have distinct values, which can be potentially distinguished in our time-resolved measurements. We only observe one fast component, which must be due to the EPC. (3) Furthermore, the fast component exists even above the magnetic transition temperature (mostly <160 K), up to room temperature and without noticeable change in the value of λ.

In summary, we have investigated the QP dynamics of $(Li_{0.84}Fe_{0.16})OHFe_{0.98}Se$ using time-resolved ultrafast spectroscopy. Under weak detection conditions, we identify the SC properties, obtaining the SC T_c and $\Delta(0)$ values. In the high fluence regime, we obtain the EPC strength $\lambda_{A_{1g}}$. Significantly, we discover a positive correlation between T_c and the EPC strength, either in the form of $\lambda_{A_{1g}}$ or λ, for all categories of iron-based superconductors. Our finding demonstrates the likely crucial role of phonon in the high temperature SC mechanism for iron-based superconductors. Our experimental results suggest the possible existence of a unified framework for understanding iron-based superconductors, including the monolayer system. Our investigation is an important step towards a unified superconducting mechanism for all iron-based superconductors.

References

[1] Hsu F C, Luo J Y, Yeh K W, Chen T K, Huang T W, Wu P M, Lee Y C, Huang Y L, Chu Y Y, Yan D C and Wu M K 2008 *Proc. Natl. Acad. Sci. USA* **105** 14262

[2] Kamihara Y, Watanabe T, Hirano M and Hosono H 2008 *J. Am. Chem. Soc.* **130** 3296

[3] Wang Q Y, Li Z, Zhang W H, Zhang Z C, Zhang J S, Li W, Ding H, Ou Y B, Deng P, Chang K, Wen J, Song C L, He K, Jia J F, Ji S H, Wang Y Y, Wang L L, Chen X, Ma X C and Xue Q K 2012 *Chin. Phys. Lett.* **29** 037402

[4] Lu X F, Wang N Z, Wu H, Wu Y P, Zhao D, Zeng X Z, Luo X G, Wu T, Bao W, Zhang G H, Huang F Q, Huang Q Z and Chen X H 2015 *Nat. Mater.* **14** 325

[5] Luo C W, Wu I H, Cheng P C, Lin J Y, Wu K H, Uen T M, Juang J Y, Kobayashi T, Chareev D A, Volkova O S and Vasiliev A N 2012 *Phys. Rev. Lett.* **108** 257006

[6] Tian Y C, Zhang W H, Li F S, Wu Y L, Wu Q, Sun F, Zhou G Y, Wang L L, Ma X C, Xue Q K and Zhao J M 2016 *Phys. Rev. Lett.* **116** 107001

[7] Gerber S, Yang S L, Zhu D, Soifer H, Sobota J A, Rebec S, Lee J J, Jia T, Moritz B, Jia C, Gauthier A, Li Y, Leuenberger D, Zhang Y, Chaix L, Li W, Jang H, Lee J S, Yi M, Dakovski G L, Song S, Glownia J M, Nelson S, Kim K W, Chuang Y D, Hussain Z, Moore R G, Devereaux T P, Lee W S, Kirchmann P S and Shen Z X 2017 *Science* **357** 71

[8] Ren Y H, Gong Y, Nosach T, Li J, Tu J J, Li L J, Cao G H and Xu Z A 2012 *J. Appl. Phys.* **111** 07E134

[9] Mansart B, Boschetto D, Savoia A, Rullier-Albenque F, Bouquet F, Papalazarou E, Forget A, Colson D, Rousse A and Marsi M 2010 *Phys. Rev. B* **82** 024513

[10] Mertelj T, Kabanov V V, Gadermaier C, Zhigadlo N D, Katrych S, Karpinski J and Mihailovic D 2009 *Phys. Rev. Lett.* **102** 117002

[11] Torchinsky D H, Chen G F, Luo J L, Wang N L and Gedik N 2010 *Phys. Rev. Lett.* **105** 027005

[12] Torchinsky D H, McIver J W, Hsieh D, Chen G F, Luo J L, Wang N L and Gedik N 2011 *Phys. Rev. B* **84** 104518

[13] Dong X L, Jin K, Yuan D N, Zhou H X, Yuan J, Huang Y L, Hua W, Sun J L, Zheng P, Hu W, Mao Y Y, Ma M W, Zhang G M, Zhou F and Zhao Z X 2015 *Phys. Rev. B* **92** 064515

[14] Sun H L, Woodruff D N, Cassidy S J, Allcroft G M, Sedlmaier S J, Thompson A L, Bingham P A, Forder S D, Cartenet S, Mary N, Ramos S, Foronda F R, Williams B H, Li X D, Blundell S J and Clarke S J 2015 *Inorg. Chem.* **54** 1958

[15] Guo J G, Jin S F, Wang G, Wang S C, Zhu K X, Zhou T T, He M and Chen X L 2010 *Phys. Rev. B* **82** 180520

[16] Zhao L, Liang A J, Yuan D N, Hu Y, Liu D F, Huang J W, He S L, Shen B, Xu Y, Liu X, Yu L, Liu G D, Zhou H X, Huang Y L, Dong X L, Zhou F, Liu K, Lu Z Y, Zhao Z X, Chen C T, Xu Z Y and Zhou X J 2016 *Nat. Commun.* **7** 10608

[17] Niu X H, Peng R, Xu H C, Yan Y J, Jiang J, Xu D F, Yu T L, Song Q, Huang Z C, Wang Y X, Xie B P, Lu X F, Wang N Z, Chen X H, Sun Z and Feng D L 2015 *Phys. Rev. B* **92** 060504

[18] Dong X L, Zhou H X, Yang H X, Yuan J, Jin K, Zhou F, Yuan D N, Wei L L, Li J Q, Wang X Q, Zhang G M and Zhao Z X 2015 *J. Am. Chem. Soc.* **137** 66

[19] Hinton J P, Thewalt E, Alpichshev Z, Mahmood F, Koralek J D, Chan M K, Veit M J, Dorow C J, Barisic N, Kemper A F, Bonn D A, Hardy W N, Liang R X, Gedik N, Greven M, Lanzara A and Orenstein J 2016 *Sci. Rep.* **6** 23610

[20] Demsar J, Podobnik B, Kabanov V V, Wolf T and Mihailovic D 1999 *Phys. Rev. Lett.* **82** 4918

[21] Wu Y L, Yin X, Hasaien J, Ding Y and Zhao J M 2020 *Chin. Phys. Lett.* **37** 047801

[22] Rothwarf A and Taylor B N 1967 *Phys. Rev. Lett.* **19** 27

[23] Kabanov V V, Demsar J and Mihailovic D 2005 *Phys. Rev. Lett.* **95** 147002

[24] Allen P B 1987 *Phys. Rev. Lett.* **59** 1460

[25] Boschetto D, Gamaly E G, Rode A V, Luther-Davies B, Glijer D, Garl T, Albert O, Rousse A and Etchepare J 2008 *Phys. Rev. Lett.* **100** 027404

[26] Brorson S D, Kazeroonian A, Moodera J S, Face D W, Cheng T K, Ippen E P, Dresselhaus M S and Dresselhaus G 1990 *Phys. Rev. Lett.* **64** 2172

[27] Wu Q, Sun F, Zhang Q Y, Zhao L X, Chen G F and Zhao J M 2020 *Phys. Rev. Mater.* **4** 064201

[28] Aku-Leh C, Zhao Jimin, Merlin R, Menendez J and Cardona M 2005 *Phys. Rev. B* **71** 205211

[29] Hu L L, Yang M, Wu Y L, Wu Q, Zhao H, Sun F, Wang W, He R, He S L, Zhang H, Huang R J, Li L F, Shi Y G and Zhao J 2019 *Phys. Rev. B* **99** 094307

[30] Sun F, Wu Q, Wu Y L, Zhao H, Yi C J, Tian Y C, Liu H W, Shi Y G, Ding H, Dai X, Richard P and Zhao Jimin 2017 *Phys. Rev. B* **95** 235108

[31] Zhao Jimin, Bragas A V, Merlin R and Lockwood D J 2006 *Phys. Rev. B* **73** 184434

[32] Yu B H, Tian Z Y, Sun F, Peets D C, Bai X D, Feng D L and Zhao J M 2020 *Opt. Express* **28** 15855

[33] A similar low-lying mode is also considered: Carbone F, Yang D S, Giannini E and Zewail A H 2008 *Pro. Natl. Acad. Sci. USA* **105** 20161

[34] Rettig L, Cortes R, Jeevan H S, Gegenwart P, Wolf T, Fink J and Bovensiepen U 2013 *New J. Phys.* **15** 083023

[35] Subedi A, Zhang L J, Singh D J and Du M H 2008 *Phys. Rev. B* **78** 134514

[36] Gnezdilov V, Pashkevich Y G, Lemmens P, Wulferding D, Shevtsova T, Gusev A, Chareev D and Vasiliev A 2013 *Phys. Rev. B* **87** 144508

[37] Jishi R A and Alyahyaei H M 2010 *Adv. Conden. Matter Phys.* **2010** 804343

[38] Um Y J, Bang Y, Min B H, Kwon Y S and Le Tacon M 2014 *Phys. Rev. B* **89** 184510

[39] Li J and Huang G Q 2013 *Solid State Commun.* **159** 45

[40] Boeri L, Dolgov O V and Golubov A A 2008 *Phys. Rev. Lett.* **101** 026403

[41] Hadjiev V G, Iliev M N, Sasmal K, Sun Y Y and Chu C W 2008 *Phys. Rev. B* **77** 220505

[42] Yndurain F 2011 *Europhys. Lett.* **94** 37001

[43] Miao R D, Bai Z, Yang J, Chen X, Cai D, Fan C H, Wang L, Zhang Q L and Chen L A 2013 *Solid State Commun.* **154** 11

[44] Choi K Y, Wulferding D, Lemmens P, Ni N, Bud'ko S L and Canfield P C 2008 *Phys. Rev. B* **78** 212503

[45] Um Y J, Park J T, Min B H, Song Y J, Kwon Y S, Keimer B and Le Tacon M 2012 *Phys. Rev. B* **85** 012501

[46] Bazhirov T and Cohen M L 2012 *Phys. Rev. B* **86** 134517

[47] Mittal R, Gupta M K, Chaplot S L, Zbiri M, Rols S, Schober H, Su Y, Brueckel T and Wolf T 2013 *Phys. Rev. B* **87** 184502

[48] Boeri L, Calandra M, Mazin I I, Dolgov O V and Mauri F 2010 *Phys. Rev. B* **82** 020506

[49] Rahlenbeck M, Sun G L, Sun D L, Lin C T, Keimer B and Ulrich C 2009 *Phys. Rev. B* **80** 064509

[50] Allen P B and Dynes R C 1975 *Phys. Rev. B* **12** 905

[51] Mcmillan W L 1968 *Phys. Rev.* **167** 331

[52] Zhang S Y, Guan J Q, Jia X, Liu B, Wang W H, Li F S, Wang L L, Ma X C, Xue Q K, Zhang J D, Plummer E W, Zhu X T and Guo J D 2016 *Phys. Rev. B* **94** 081116

[53] Avigo I, Cortes R, Rettig L, Thirupathaiah S, Jeevan H S, Gegenwart P, Wolf T, Ligges M, Wolf M, Fink J and Bovensiepen U 2013 *J. Phys. Conden Matter* **25** 094003

[54] Parker D R, Pitcher M J, Baker P J, Franke I, Lancaster T, Blundell S J and Clarke S J 2009 *Chem. Commun.* **16** 2189

[55] Katayama N, Ji S D, Louca D, Lee S, Fujita M, Sato T J, Wen J S, Xu Z J, Gu G D, Xu G Y, Lin Z W, Enoki M, Chang S, Yamada K and Tranquada J M 2010 *J. Phys. Soc. Jpn.* **79** 113702

[56] Tapp J H, Tang Z J, Lv B, Sasmal K, Lorenz B, Chu P C W and Guloy A M 2008 *Phys. Rev. B* **78** 060505